Journal of Gastrointestinal Surgery (2019) 23:2174–2183
https://doi.org/10.1007/s11605-019-04130-2

ORIGINAL ARTICLE

Comprehensive Characterization of a Porcine Model of The "Small-for-Flow" Syndrome

Maitane I. Orue-Echebarria[1,2] · Javier Vaquero[3] · Cristina J. Lisbona[4] · Pablo Lozano[1] · Miguel A. Steiner[1] · Álvaro Morales[1] · José Á. López-Baena[1] · Juan Laso[4] · Inmaculada Hernández[4] · Luis Olmedilla[4] · José L. García Sabrido[1] · Isabel Peligros[5] · Emma Sola[5] · Carlos Carballal[6] · Elena Vara[7] · J. M. Asencio[1,2,8]

Received: 11 November 2018 / Accepted: 16 January 2019 / Published online: 7 February 2019

Abstract

Introduction The term "Small-for-Flow" reflects the pathogenetic relevance of hepatic hemodynamics for the "Small-For-Size" syndrome and posthepatectomy liver failure. We aimed to characterize a large-animal model for studying the "Small-for-Flow" syndrome.

Methods We performed subtotal (90%) hepatectomies in 10 female MiniPigs using a simplified transection technique with a tourniquet. Blood tests, hepatic and systemic hemodynamics, and hepatic function and histology were assessed before (Bas), 15 min (t-15 min) and 24 h (t-24 h) after the operation. Some pigs underwent computed tomography (CT) scans for hepatic volumetry ($n = 4$) and intracranial pressure (ICP) monitoring ($n = 3$). Postoperative care was performed in an intensive care unit environment.

Results All hepatectomies were successfully performed, and hepatic volumetry confirmed liver remnant volumes of 9.2% [6.2–11.2]. The hepatectomy resulted in characteristic hepatic hemodynamic alterations, including portal hyperperfusion, relative decrease of hepatic arterial blood flow, and increased portal pressure (PP) and portal-systemic pressure gradient. The model reproduced major diagnostic features including the development of cholestasis, coagulopathy, encephalopathy with increased ICP, ascites, and renal failure, hyperdynamic circulation, and hyperlactatemia. Two animals (20%) died before t-24 h. Histological liver damage was observed at t-15 min and at t-24 h. The degree of histological damage at t-24 h correlated with intraoperative PP ($r = 0.689$, $p = 0.028$), hepatic arterial blood flow ($r = 0.655$, $p = 0.040$), and hepatic arterial pulsatility index ($r = 0.724$, $p = 0.066$). All animals with intraoperative PP > 20 mmHg presented liver damage at t-24 h.

Conclusion The present 90% hepatectomy porcine experimental model is a feasible and reproducible model for investigating the "Small-for-Flow" syndrome.

Keywords Small-for-Size · Hepatectomy · Pig · Small-For-Flow · Posthepatectomy liver failure

✉ J. M. Asencio
jmasencio@gmail.com

[1] Transplant and Hepatobiliopancreatic Surgery Unit, Department of General and Digestive Surgery, Hospital General Universitario Gregorio Marañón - IiSGM, Madrid, Spain

[2] Department of Surgery, School of Medicine, Universidad Complutense de Madrid, Madrid, Spain

[3] Research Laboratory in Hepatology and Gastroenterology, Hospital General Universitario Gregorio Marañón - IiSGM – CIBERehd, Madrid, Spain

[4] Department of Anaesthesiology and Resuscitation, Hospital General Universitario Gregorio Marañón - IiSGM, Madrid, Spain

[5] Department of Pathology, Hospital General Universitario Gregorio Marañón - IiSGM, Madrid, Spain

[6] Department of Neurosurgery, Hospital General Universitario Gregorio Marañón - IiSGM, Madrid, Spain

[7] Department of Biochemistry and Molecular Biology, School of Medicine, Universidad Complutense de Madrid, Madrid, Spain

[8] Department of General Surgery, Hospital General Universitario Gregorio Marañón - IiSGM, c/ Doctor Esquerdo 46, 28007 Madrid, Spain

Introduction

The concept of "Small-for-Flow" syndrome arises from the observation that the determining factor of the appearance of the "Small-for-Size" syndrome (SFSS) and the posthepatectomy liver failure (PHLF) *may be* the increase of portal inflow against a reduced hepatic mass.[1–6] The increase in portal blood flow (PBF) relative to the remnant liver leads to portal hypertension and to decreased hepatic arterial blood flow (HABF) due to the hepatic artery buffer response. The mismatch between PBF and sinusoidal mass induces a series of structural alterations that trigger subsequent changes in inflammatory mediators. These alterations impair the regenerative capacity of the liver parenchyma and reduce its energy load, ultimately impeding to fulfill metabolic and synthetic requirements.[7,8]

Based on studies where hepatic hemodynamics were modulated in hepatic surgeries,[9–12] the "Small-for-Flow" syndrome would be defined by the following intraoperative criteria: a portal pressure (PP) greater than 20 mmHg or a PBF greater than 250 ml/min/100 g.[13] Surpassing of these thresholds would indicate the need to take measures for preventing the structural alterations caused by the inflow imbalance, setting a scenario for the future development of such interventions. In addition, this approach would allow the evaluation of the effectiveness of potential interventions in real time. Because clinical trials in this field are limited by high morbidity and mortality and by ethical considerations, it is necessary to establish experimental models that reproduce the human condition. Porcine models of subtotal hepatectomies are particularly valuable, as their anatomy and physiology are similar to humans.[14,15] These large animals allow the measurement of portal and arterial blood flows and pressures intraoperatively,[16,17] as well as the exploration of potential maneuvers to expand the safety limits in liver surgery.[18]

The aim of the present work was to characterize a large animal model in which all the features that characterize the "Small-for-Size" syndrome and the postoperative liver failure can be recapitulated, therefore providing relevant endpoints for studying its pathogenesis and testing therapeutic interventions.

Materials and Methods

Ten female MiniPigs (body weight 42 kg [39.2–49.7], length 132 cm [119–150]) were anesthetized and underwent the following protocol (Fig. 1). Briefly, an intracranial pressure (ICP) measurement sensor was placed in three animals, and a cranial and abdominal computed tomography (CT) scan were then performed. An abdominal CT scan was also performed in a fourth animal without ICP monitoring. Back in the operating room, blood vessels were cannulated and a 90% hepatectomy with hemostatic control was performed.[19] The laparotomy was closed, and the animal was transferred to the radiology room to perform a new cranial and abdominal CT scan if indicated. Once the studies were completed, the animals remained monitored under observation with invasive respiratory support until they were sacrificed 24 h later. The measurement of hemodynamic and liver function parameters, and the collection of blood samples and liver biopsies were performed at the beginning of the surgery (Bas), 15 min after the subtotal hepatectomy (t-15 min) when the animals were hemodynamically stable, and 24 h after surgery (t-24 h) (Fig. 1).

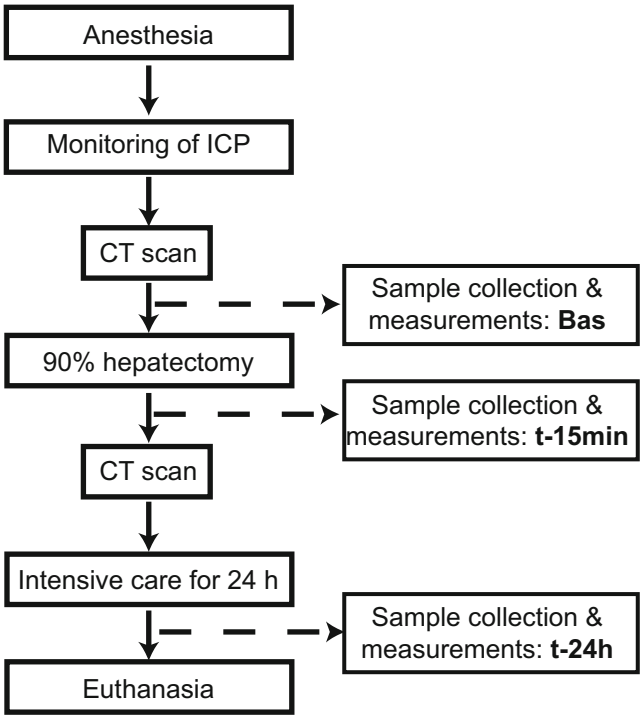

Fig. 1 Flow chart showing the experimental design and the timing of the main procedures carried out during the surgical intervention and the postoperative follow-up

The study was approved by the Ethics Committee for Animal Experimentation of the Minimally Invasive Surgery Center Jesús Usón (CCMIJU) in Cáceres, Spain. All experiments were performed in compliance with the "Guide for the care and use of laboratory animals" by the American Research Council, 2011 edition (https://www.nap.edu/download/12910) and the ARRIVE guidelines. At the end of the study protocol or when ethically indicated, the animals were sacrificed under deep anesthesia with intravenous injection of propofol (200 mg) followed by potassium chloride (2 mmol/kg). The specific clinical and behavioral signs used as endpoint criteria to indicate the euthanasia were the following: severe hepatic insufficiency, hyperactivity, and respiratory insufficiency with O2 saturation < 85%.

Anesthesia Protocol

All animals underwent surgery under general anesthesia following a standard protocol. Briefly, animals received a patch of fentanyl and were fasted with free access to water 24 h before the operation. The next morning, pigs were first premedicated with ketamine 15 mg/kg i.m. Once sedated, they were transferred to the operating room, their weight and length were recorded, a thermal blanket was placed to avoid hypothermia and a peripheral vein in the ear was cannulated with a 20-22G tube. After preoxygenation with 100% oxygen, general anesthesia was induced with fentanyl (3 μg/kg i.v.), propofol (2–4 mg/kg i.v.), and atracurium (0.6 mg/kg i.v.). Subsequently, an intratracheal tube and a nasogastric tube were placed to facilitate the surgical procedure. Fluid therapy was performed with an i.v. infusion of 6–8 ml/kg/h of crystalloids. The colloid hydroxyethyl starch (Voluven®) was added when needed to maintain hemodynamic stability. If hypotension (MAP < 60 mmHg) occurred despite fluid therapy, intravenous boluses of ephedrine 5 mg or phenylephrine 0.1 mg were added to maintain MAP equal to or greater than 60 mmHg. After the hepatectomy, glycemia was hourly measured and a 10% glucose solution was administered to maintain glycemia over 100 mg/dl.

Measurement of Systemic and Hepatic Hemodynamics

Once anesthetized, the initial monitoring consisted of a one-lead electrocardiogram, pulse oximetry, capnography, and FiO2. A femoral artery was canalized with a PICCO® catheter, and the PiCCO2® monitor (Pulsion Medical System AG, Munich, Germany) was used for advanced hemodynamic monitoring. The central venous pressure (CVP) was measured through a bilumen catheter inserted into the jugular vein. The portal pressure (PP) was measured by direct puncture of the portal vein with a 25G needle connected to a pressure transducer (Fig. 2a), and the portal blood flow (PBF) and the hepatic arterial blood flow (HABF) were measured with a flow-meter per transit time probe (MediStim® AS, Oslo, Norway) (Fig. 2b). Portal-systemic pressure gradient (PSPG) was calculated as the difference between the CVP and PP. Other calculated variables included the HABF corrected by liver weight (HABF per 100 g), the PBF corrected by liver weight (PBF per 100 g), the total hepatic blood flow (THBF), the hepatic artery pulsatility index (PIa), the percentage of THBF that depends on the hepatic artery (HABF/THBF), and the percentage of THBF that depends on the portal vein (PBF/THBF).

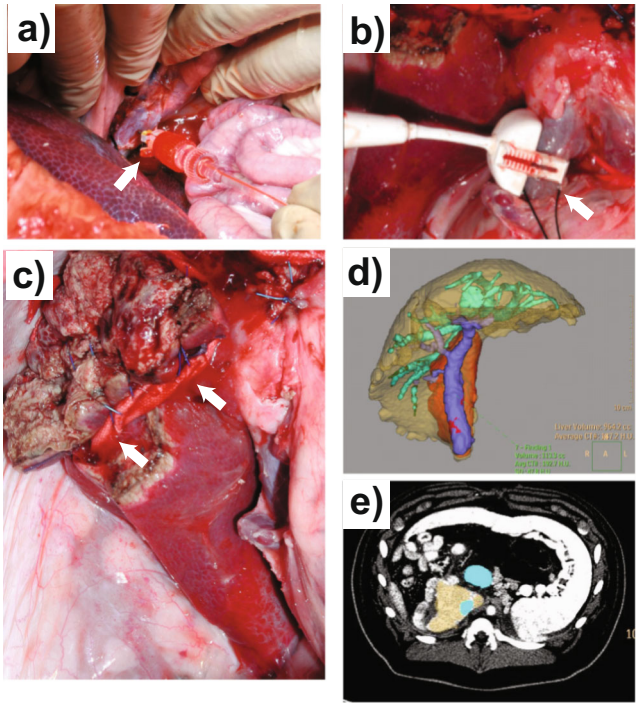

Fig. 2 Surgery and hepatic volumetry. The panels show representative images of the measurement of **a** the portal pressure (PP) (white arrow) and **b** the portal blood flow (PBF) (white arrow) before the hepatectomy using a flow-meter per transit time. **c** The hepatic remnant representing 10% of the initial liver mass, including the tourniquet used for the hepatic resection (white arrows), **d** reconstruction of the total hepatic volume including the liver mass planned to be resected (light brown), the estimated liver remnant (orange), and the volume occupied by vessels (light green) in a computerized tomography image used for hepatic volumetry, and **e** a computerized tomography image showing the liver remnant (light brown) and the big vessels (bright blue) after the hepatectomy

Surgical Procedure for Resecting 90% of Liver Mass

Animals were placed in supine position, draped in a sterile fashion and a J laparotomy was performed. After mobilization of the falciform ligament, dissection was carried out to expose the hepatic hilum. The portal vein and the hepatic artery were then dissected and isolated with a vessel loop to facilitate its identification during surgery, but no Pringle maneuver was performed. The hepatic resection consisted of a 90% hepatectomy following the technique described by Xia et al.,[20] except that a tourniquet was used to improve hemostasia as described by Kahn et al..[21] Briefly, the falciform ligament, the left triangular ligament, and the lesser omentum were cut to allow the identification of hepatic veins and the mobilization of left liver lobes. Afterwards, an in-block resection of the left lateral (LLL), left medial (LML), and right medial (RML) lobes was performed by placing a tourniquet around the parenchyma at the origin of the three left lobes, which was fixed with interrupted prolene stitches of 1/0 and hemostasis suture with prolene threads of 0/0 resting on the tourniquet tape, and the transection was performed using Ligasure and EndoGIA

(Covidien, Minneapolis, MN), (Fig. 2c). Subsequently, the 90% hepatectomy was completed with the resection of the right lateral lobe (RLL). After confirming adequate hemostasis, the abdominal cavity was washed with sterile 0.9% saline, and the t-15 min measurements were taken. Finally, the laparotomy was closed in two levels with non-absorbable suture.

Measurement of Liver Function

Liver function was assessed by the indocyanine green (ICG) clearance test measured with the PiCCO2® monitor. It was expressed using the plasma disappearance rate per minute (PDR) and the retention rate at 15 min (R15) after an intravenous injection of 0.5 mg/kg of ICG.

Intracranial Pressure Monitoring

Intracranial pressure monitoring was performed by introducing an intraparenchymal brain sensor (Camino® Integra®) in three of the animals.[22] Before and after surgery, a cranial CT scan was performed to assess the position of the sensor and the presence of signs of cerebral edema.[23] Boluses of pentothal (1–4 mg/kg) or mannitol 20% (0.25 a 1 g/kg/ 2–6 h) were administered when ICP increased over 20 mmHg.

Liver Volumetry

An abdominal CT scan with i.v. contrast was performed before and after the hepatectomy in four animals. The total hepatic volume and the estimated liver remnant volume were calculated on CT images (Philips CT Scanner Brilliance 6 slice). The calculation of the hepatic volumes was performed with a liver segmentation program (Philips Intellispace Portal) (Fig. 2d, e).

Histological Evaluation

Liver tissue samples were fixed in 10% buffered formalin and paraffin-embedded. Histological sections (6 μm thick) of liver tissue were stained with hematoxylin-eosin and Masson's trichrome, and evaluated blindly by two pathologists (IP, ES). A score of histological damage was elaborated from 7 parameters: congestion, hemorrhage, periportal edema, septal edema, endothelial detachment, necrosis, and apoptosis. Each parameter was scored no damage (0), low (1), moderate (2), and severe (3). The final Histological Damage Score was calculated as ∑(congestion + 2 × hemorrhage + periportal edema + septal edema + 2 × endothelial detachment + 2 × necrosis + 2 × apoptosis), in order to give more weight to the parameters reflecting more severe damage. Therefore, the score ranged from 0 to 33 points, considering histological damage a score ≥ 3.

Statistical Analysis

Quantitative variables were expressed as median [interquartile range] and qualitative variables as percentage (%). Differences between time points (Bas vs. t-15 min, and Bas vs. t-24 h) were evaluated using paired *t* tests applying the Bonferroni correction for multiple comparisons. Correlations between two variables were assessed by Pearson test. A p value < 0.05 was considered statistically significant. The statistical analysis was performed using the SPSS version 20.0 (IBM Corporation, Armonk, NY) and Prism 7 for Windows (GraphPad Software, Inc).

Results

The 90% hepatectomy was completed successfully in all the animals, and all of them were hemodynamically stable at the end of the surgery. Body temperature slightly decreased during surgery (Bas, 36.9 °C [36.0–37.9] vs. t-15 min, 36.4 °C [35.0–37.1]; $p = 0.004$), but it recovered at 24 h (35.8 °C [35.2–37.5], $p = 1.0$ vs. Bas).

Surgery, Clinical Course, and Survival of Pigs Undergoing 90% Hepatectomy

The hepatectomy reduced the weight of the liver from 956 g [882–1019] (summing up the weights of the resected lobes, plus the liver remnant at sacrifice) to 168 g [140–182] (weight of the liver remnant at sacrifice) ($p < 0.0001$ Bas vs. t-24 h); calculated in this manner, the liver remnant represented 18.2% [14.3–19.1] of the total liver weight. Because the congestion and edema of the liver remnant may increase its weight when measured at 24 h, we performed CT scans in four animals before and immediately after the hepatectomy in order to determine the exact percentage of resection of liver mass. In these animals, the total liver volume was reduced from 1248 cc [1163–1474] at Bas to 129 cc [78–140] after the surgery ($p = 0.0006$), which represented 9.2% [6.2–11.2] of the initial liver volume (Fig. 2d, e).

Three animals underwent ICP monitoring, and in all of them ICP increased during the postoperative period (Fig. 3). One of the animals presented an increase of ICP from 10 mmHg at 3 h to 40 mmHg at 6 h, and died shortly thereafter. A second animal (without ICP monitoring) died at 12 h after the surgery due to a cardiac thrombotic complication. The remaining eight animals survived for 24 h. Of the ten animals, eight of them (80%) presented ascites at the necropsy.

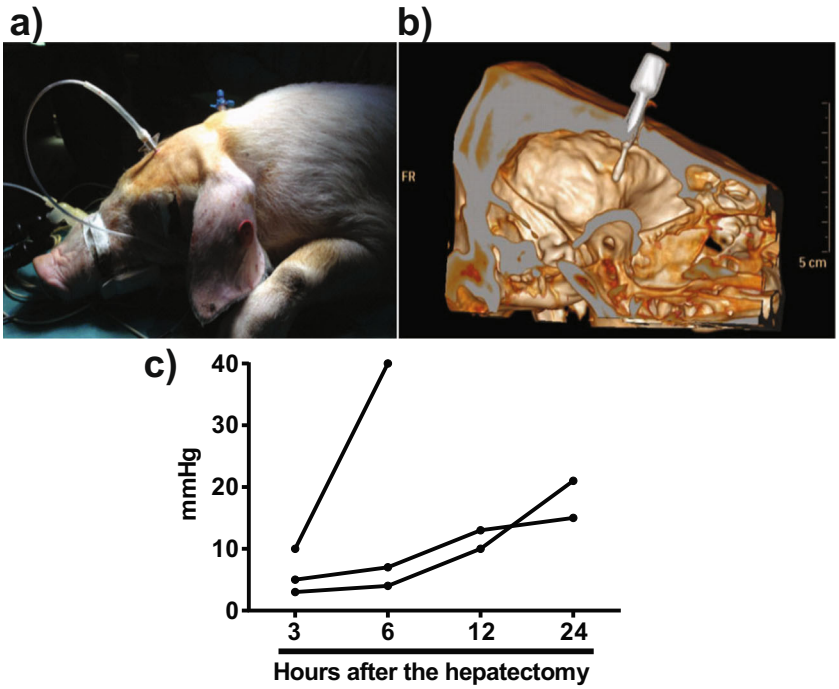

Fig. 3 Measurement of intracranial pressure (ICP). The panels show representative images of **a** the placement of an intracranial pressure sensor in a pig, **b** a cranial computed tomography reconstruction verifying the position of the intracranial pressure sensor, and **c** the evolution of ICP after a 90% hepatectomy in the three animals undergoing ICP monitoring

Blood Laboratory Parameters

Compared with baseline measurements, the 90% hepatectomy resulted in some changes of blood laboratory parameters immediately after the surgery (t-15 min) and more extensive alterations 24 h later (t-24 h) (Table 1). The earliest alterations included decreases of the platelet count ($p = 0.006$), GGT ($p < 0.001$), and albumin ($p = 0.030$), and increases of glycemia ($p = 0.040$), AST ($p = 0.006$) and lactate ($p = 0.004$), which was associated with a trend to a lower pH ($p = 0.064$). At the 24-h time point, the animals presented decreases of hemoglobin ($p = 0.002$), hematocrit ($p = 0.003$), and albumin ($p = 0.023$), and increases of AST ($p = 0.035$), bilirubin ($P = 0.007$), AP ($p = 0.009$), and creatinine ($p = 0.017$). At this time point, the animals also presented coagulopathy (increase of prothrombin time ($p = 0.002$) and INR ($p < 0.001$)) and a persistent increase of blood lactate ($p = 0.042$).

Systemic Hemodynamic Parameters

All pigs remained hemodynamically stable early after the surgery (t-15 min), although they showed a trend to increase the heart rate (HR, $p = 0.080$) and the systolic volume index (SVI, $p = 0.067$) (Table 2). Twenty-four hours after the surgery, the pigs developed a hyperdynamic circulation with increased cardiac index (CI, $p = 0.039$) and HR ($p = 0.012$) and decreased mean arterial pressure (MAP, $p = 0.027$) and systemic vascular resistance index (SVRI, p = 0.039), as well as a trend to an increase of the cardiac function index (CFI, $p = 0.097$) (Table 2). Of note, no changes were observed at any time point in other general hemodynamic parameters such as the central venous pressure (CVP), the global end-diastolic volume index (GEDI), the maximum rate of increase of arterial pressure (Dpmax), or the stroke volume variation (SVV), nor in hemodynamic parameters of the pulmonary circulation such as the extra vascular lung water index (ELWI).

Hepatic Hemodynamic Parameters

The 90% hepatectomy resulted in dramatic changes of hepatic hemodynamic parameters (Fig. 4). The resection of liver mass was accompanied by an immediate decrease of the THBF (Bas, 1030 mL/min [769–1165] vs. t-15 min, 398 mL/min [279–599]; $p < 0.001$), which resulted from a decrease of both the HABF (195 mL/min [171–490] vs. 45 mL/min [29–66], $p = 0.006$) and the PBF (585 mL/min [471–823] vs. 355 mL/min [240–566], $p = 0.044$). The changes of the HABF and the PBF, however, did not occur in the same proportion, resulting in a decrease of the HABF relative to the THBF (26% [21–46] vs. 10%,[7–18] $p = 0.015$) with a corresponding relative increase of the PBF (Fig. 4a, b). Although the absolute values of hepatic blood flows were reduced, the hepatectomy resulted in relative hyperemia of the liver remnant, as shown by the marked increase of the PBF, but not of the HABF, relative to liver mass (PBF, Bas, 61 mL/min/100 g [53–87] vs. t-15 min, 204 mL/min/100 g [154–322]; $p = 0.003$; HABF, 21 ml/min/100 g [19–51] vs. 25 ml/min/100 g [21–40]; $p = 0.97$) (Fig. 4a, b). As a direct consequence of the relative hyperemia, the portal pressure (PP) increased immediately after the resection in all the animals (9.0 mmHg [7.0–13.5] vs. 22.0 mmHg

Table 1 Blood laboratory parameters at baseline (Bas), 15 min (t-15 min), and 24 h (t-24 h) after a 90% hepatectomy in pigs

	Baseline	t-15 min	*p**	t-24 h	*p#*
Hemoglobin (g/dl)	9.9 [8.6–10.9]	8.7 [8.3–9.8]	0.144	7.1 [6.5–7.7]	**0.002**
Hematocrit (%)	30.3 [26.8–33.4]	26.3 [24.8–28.8]	0.184	22.6 [19.9–23.4]	**0.003**
Platelets (10^3μL)	350 [278–484]	311 [254–414]	**0.006**	241 [209–287]	0.188
Leukocytes (10^3μL)	19.0 [15.1–23.2]	14.6 [11.3–24.5]	1.0	28.5 [9.9–46.5]	0.206
PT (seg)	14.2 [9.5–14.9]	12.6 [9.8–14.9]	1.0	23.7 [19.7–26.4]	**0.002**
INR	0.93 [0.79–0.96]	0.93 [0.83–1.00]	0.304	1.96 [1.60–2.25]	< **0.001**
APTT (seg)	18.2 [16.9–23.4]	16.6 [16.4–17.3]	0.106	21.3 [18.3–38.8]	0.320
Glucose (mg/dL)	110 [87–148]	186 [142–230]	**0.040**	147 [87–370]	0.426
ALT (UI/L)	45 [34–55]	36 [28–51]	0.429	72 [41–115]	0.216
AST (UI/L)	62 [53–81]	98 [74–149]	**0.006**	539 [321–717]	**0.035**
Bilirubin (mg/dL)	0.40 [0.15–0.55]	0.40 [0.25–0.70]	0.191	1.70 [1.40–2.10]	**0.007**
GGT (UI/L)	42 [31–47]	34 [18–37]	< **0.001**	40 [26–60]	0.381
AP (UI/L)	265 [120–362]	258 [98–318]	0.714	611 [374–1133]	**0.009**
LDH (UI/L)	1117 [681–1470]	1039 [574–1553]	1.0	2175 [1776-3446]	0.167
Albumin (g/dL)	2.40 [2.25–2.60]	1.95 [1.80–2.10]	**0.030**	2.05 [1.70–2.73]	**0.023**
Creatinine (mg/dL)	1.29 [0.68–2.13]	1.29 [0.79–2.14]	1.0	1.44 [1.09–3.97]	**0.017**
Urea (mg/dL)	30.5 [19.5–34.8]	24.0 [18.5–32.0]	0.352	22.0 [21.0–36.0]	1.0
Arterial pH	7.47 [7.45–7.55]	7.42 [7.35–7.47]	0.064	7.44 [7.37–7.46]	0.373
Lactate (mmol/L)	1.5 [1.1–1.6]	3.3 [3.1–3.7]	**0.004**	4.6 [3.4–7.4]	**0.042**

*t-15 min vs. Bas, # t-24 h vs. Bas. *P* values that are statistically significant or close to significance are shown in bold

ALT alanine aminotransferase, *AP* alkaline phosphatase, *APTT* activated partial thromboplastin time, *AST* aspartate aminotransferase, *GGT* gamma glutamyltransferase, *INR* international normalized ratio, *LDH* lactate dehydrogenase, *PT* prothrombin time

[17.3–24.0], $p < 0.001$), with most of them ($n = 9$, 90%) presenting a PP above 15 mmHg (Fig. 4c). The portal-systemic pressure gradient (PSPG) also increased accordingly (3.0 mmHg [3.0–4.5] vs. 15.0 mmHg [11.0–17.8], $p < 0.001$). Both the PP ($r = -0.794$, $p = 0.006$) and the PSPG ($r = -0.732$, $p = 0.016$) were negatively correlated with the PBF. Interestingly, the PIa increased at this early time point (0.50 [0.38–0.90] vs. 4.30 [2.70–4.50], $p = 0.001$).

Most hepatic hemodynamic alterations, but not all, persisted at 24 h. Thus, THBF recovered (800 ml/min [502–1041], $p = 0.488$ vs. Bas), mostly due to the recovery of PBF (690 ml/min [443–1000], $p = 1.0$), while HABF tended to

Table 2 Systemic hemodynamic parameters at baseline (Bas), 15 min (t-15 min), and 24 h (t-24 h) after a 90% hepatectomy in pigs

	Baseline	t-15 min	*p**	t-24 h	*p#*
HR (bpm)	85 [73–112]	124 [98–133]	**0.080**	140 [103–144]	**0.012**
MAP (mmHg)	86 [68–112]	81 [68–90]	0.353	66 [35–83]	**0.027**
CVP (mmHg)	5.0 [3.5–7.8]	5.5 [2.8–10.5]	1.0	7.0 [5.0–10.0]	1.0
CI (l/min/m^2)	2.98 [2.64–3.41]	2.76 [1.78–3.26]	1.0	3.44 [3.11–4.76]	**0.039**
CFI (l/min)	6.60 [4.38–7.53]	7.60 [6.95–8.85]	0.348	8.80 [6.45–13.35]	**0.097**
SVRI (dyn*s*cm^{-5} m^2)	2368 [1633-2784]	2424 [1958-2806]	1.0	1302 [1090-1664]	**0.039**
GEDI (ml/m^2)	539 [448–749]	425 [297–480]	1.0	458 [330–516]	0.482
SVI (ml/m^2)	34.0 [27.5–47.0]	21.0 [11.5–29.0]	**0.067**	29.0 [25.3–45.0]	0.597
SVV (%)	24.5 [16.3–30.5]	20.5 [16.3–24.8]	0.282	23.0 [10.5–27.8]	1.0
Dpmax (mmHg/seg)	532 [310–623]	624 [275–831]	0.457	595 [380–960]	1.0
ELWI (ml/Kg)	12.00 [8.50–16.50]	11.00 [9.00–25.00]	0.655	13.00 [11.00–15.00]	1.0

*t-15 min vs. Bas, # t-24 h vs. Bas. *P* values that are statistically significant or close to significance are shown in bold

CI cardiac index, *CFI* cardiac function index, *Dpmax* maximum rate of increase in arterial pressure, *ELWI* extra vascular lung water index, *GEDI* global end-diastolic volume index, *HR* heart rate, *MAP* mean arterial pressure, *SVRI* systemic vascular resistance index, *SVV* stroke volume variation, *SVI* systolic volume index

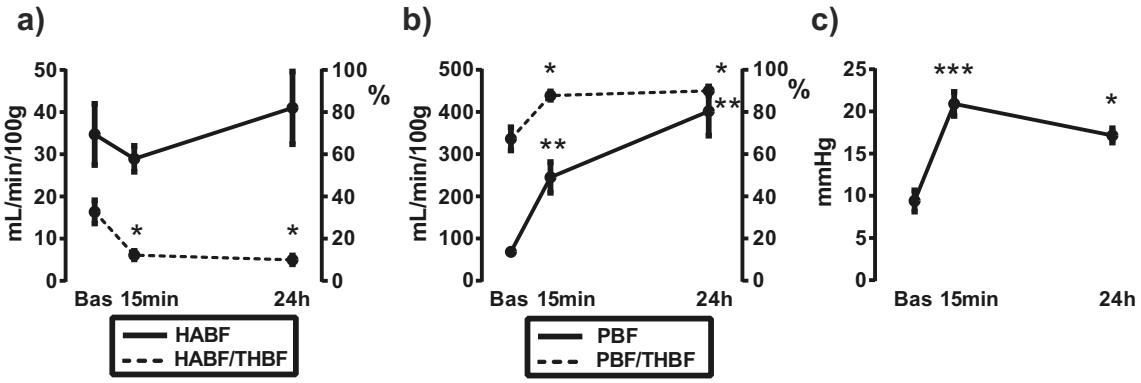

Fig. 4 Hepatic hemodynamics in pigs undergoing a 90% hepatectomy. The graphs show the values at baseline (Bas), 15 min, and 24 h after the surgery of **a** the hepatic arterial blood flow relative to liver weight (HABF, solid line, left axis) and as percentage of the total hepatic blood flow (HABF/THBF, dotted line, right axis), **b** the portal blood flow relative to liver weight (PBF, solid line, left axis) and as percentage of the THBF (PBF/THBF, dotted line, right axis), and **c** the portal pressure. Mean ± SEM. *$p < 0.05$, **$p < 0.01$, and ***$p < 0.001$ vs. Bas

remain decreased (59 ml/min [42–105], $p = 0.069$ vs. Bas). Still, the relative contributions of the HABF and the PBF to the THBF remained below (11%[4–13]) and above (89% [87–96]), respectively, compared with baseline values (both $p = 0.035$ vs. Bas) (Fig. 4a, b). Consequently, the relative portal hyperemia of the liver remnant further increased 24 h after the surgery (PBF, 399 ml/min/100 g [257–550], $p = 0.005$ vs. Bas) (Fig. 4b), and the PP (17.5 mmHg [15.5–18.5], $p = 0.014$ vs. Bas) (Fig. 4c) and the PSPG (10.0 mmHg [7.5–14.3], $p = 0.004$ vs. Bas) also remained elevated.

Liver Function

Liver function markedly worsened immediately after the hepatectomy, as shown by the decrease of PDR (Bas, 10.0 [8.1–16.5] vs. t-15 min, 4.2 [2.8–5.4]; $p = 0.027$) and the increase of R15 (Bas, 20.8 [4.7–26.0] vs. t-15 min, 53.3 [44.5–65.7]; $p = 0.003$) (Fig. 5a, b). Importantly, liver dysfunction persisted at the 24 h time point (PDR, 3.7 [3.2–4.6], $p = 0.018$ vs. Bas; R15, 57.4 [50.2–61.9], $p = 0.002$ vs. Bas).

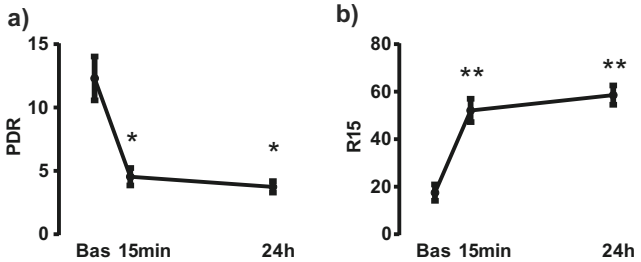

Fig. 5 Liver function in pigs undergoing a 90% hepatectomy. The graphs show the evolution of liver function at baseline (Bas), 15 min, and 24 h after the surgery evaluated by using the indocyanine green test to determine: **a** the plasma disappearance rate (PDR) and **b** the retention-15 (R15) parameter. Mean ± SEM. *$p < 0.05$ and **$p < 0.01$ vs. Bas

Histological Examination

Hepatic damage, as assessed by the Histological Damage Score, increased from 0.0 [0.0–1.25] to 5.5 [3–5–7.25] at t-15 min ($p = 0.002$ vs. Bas) and to 3.0 [1–0–6.75] at t-24 h ($p = 0.028$ vs. Bas). The histological changes at 24 h after surgery were positively correlated with the PP ($r = 0.689$ [0.105, 0.920], $p = 0.028$, Fig. 6a) and the HABF per 100 g of liver tissue ($r = 0.655$ [0.042, 0.909], $p = 0.040$, Fig. 6b) and inversely with the PIa ($r = -0.724$ [−0.956, 0.065], $p = 0.066$, Fig. 6c), all of them measured immediately after the resection of liver mass. Noteworthy, all animals with a PP above 20 mmHg early after the surgery showed histological damage (score ≥ 3) 24 h later (Fig. 6a).

Discussion

Establishing a preclinical model in a large experimental animal is crucial for increasing the understanding of the underlying mechanisms of the "Small-for-Size" syndrome and the posthepatectomy liver failure. In the present study, we characterized a model consisting of the resection of 90% of the hepatic parenchyma in pigs using a simplified and reproducible surgical technique and a comprehensive monitoring protocol. Remarkably, the model replicated the major analytical, hemodynamic, functional, and histological features of the "Small-for-Size" syndrome and posthepatectomy liver failure, as well as their extra-hepatic complications and mortality.

The "Small-for-Size" syndrome, resulting from the transplantation of liver grafts that are too small, and the posthepatectomy liver failure, resulting from excessive resections of liver mass, are both clinical entities characterized by the development of liver failure manifested as cholestasis, coagulopathy, encephalopathy, and ascites, frequently leading

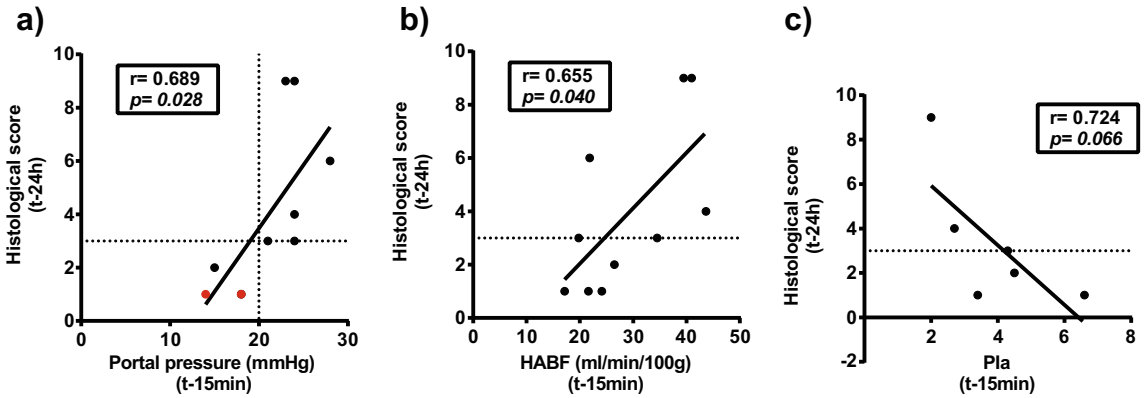

Fig. 6 Hepatic hemodynamic determinants of liver damage. The graphs show the relationship of the histological damage score evaluated 24 h after the surgery with **a** the portal pressure, **b** the hepatic arterial blood flow (HABF) relative to liver weight, and **c** the pulsatility index of the hepatic artery (PIa), all of them measured immediately after the hepatic resection (t-15 min). **a**–c The dotted lines at $y = 3$ represent the value above which animals were considered to have histological damage. In **a**, a dotted line is also shown at $x = 20$ mmHg. The correlation between variables was evaluated by Pearson's test, and the solid lines represent the linear regression lines

to multi-organ failure and death.[24–26] Here, we confirmed that pigs undergoing a 90% hepatectomy developed liver damage and dysfunction, as well as alterations in other organs such as the brain and kidneys. The development of liver damage was reflected analytically by early increases of transaminases in plasma accompanied by cholestasis (increased bilirubin and AP) 24 h after the surgery. The peak of liver enzymes was lower in comparison with the reported in a porcine model of transplantation of small-size grafts, probably because of the additional deleterious effects of ischemia-reperfusion damage in the later.[16] Liver damage was also confirmed histologically by the presence of characteristic alterations, which included sinusoidal congestion, periportal and periseptal edema, and perisinusoidal hemorrhage.[27,28] The development of liver dysfunction was supported by the appearance of coagulopathy (increased INR and PT) and hypoalbuminemia, and by the decrease of PDR and increase R15 of indocyanine green, which have been similarly reported in pigs undergoing transplantation of small-size liver grafts.[16] The decrease of liver function was observed almost immediately after the resection of liver mass and it persisted at the 24-h time point, when ascites was also noted in most of the animals. Finally, we also observed the following extra-hepatic alterations: (i) the increase of creatinine suggestive of kidney failure, (ii) the progressive increases of ICP refractory to mannitol and pentothal in the 3 individual animals undergoing ICP monitoring (leading to early death by brain herniation in one of them), resembling findings reported in pigs undergoing total hepatectomies,[23] and (iii) the development of hyperdynamic circulation (increased heart rate, CI and CFI, and decreased MAP and SVRI) and hyperlactatemia, which are commonly observed in patients with acute liver failure. In summary, the present model reproduced the most common alterations that define the syndromes of "Small-for-Size" and posthepatectomy liver failure.

Rather than renaming the previous clinical entities, the term "Small-for-Flow" syndrome aims to reflect the crucial role of hepatic hemodynamics for the development of liver failure in hepatic surgeries. A major strength of the present model was the reproduction of such alterations, which included the portal hyperperfusion of the liver remnant, the relative decrease of HABF, and the increase of PP and PSPG. Of note, these alterations developed in the setting of stable physiological parameters (glycemia, arterial blood gases) and of the hyperdynamic circulation that frequently accompanies liver failure. These observations enhance the preclinical value of the model, which allows a thorough evaluation of the effects of potential interventions for preventing/treating the "Small-for-Size" syndrome and the postoperative liver failure. Both the PBF and the PP (or the PSPG) are important parameters to assess the hemodynamic stress of the liver remnant or liver graft. Although PSPG avoids the influence of central venous pressure in the calculation and has been reported to correlate better with PBF than PP,[29] both PP and PSPG were significantly correlated with PBF in our study. Importantly, our results suggest that "pressure" parameters are preferable to "flow" parameters for predicting the extent of the liver damage. Of note, absolute blood flow (ml/min) is not fully informative because the normal value varies with the body mass of the individual and, therefore, a specific threshold is unlikely to be universally valid for all patients. Additionally, blood flow per liver mass (ml/min/100 g) is only available in the case of liver grafts, but not in the case of hepatic resections as the weight of the liver remnant is unknown. As revealed in the present study by the discordance with the volumetric evaluation, the weight of the liver remnant several hours after the surgery did not reflect the original weight, probably due to the influence of ongoing edema and congestion. Because of this reason, the values of blood flow per 100 g of liver tissue in the present study were probably slightly underestimated. Contrary to "flow"

parameters, the "pressure" parameters (PP or PSPG) may directly reflect the adequacy of blood flow and the accommodating capacity of the liver remnant regardless of the remaining liver mass or the body mass of the individual. In agreement with this notion, PP was directly correlated with the histological damage score, and all animals presenting PP above 20 mmHg immediately after the resection developed liver injury 24 h later. Finally, the HABF per 100 g and the PIa, an indicator of the difficulty of the arterial blood to cross the sinusoid, were also correlated with the degree of histological damage. These measurements, which can be easily measured with a flow-meter probe, could thus be helpful for improving the prediction of liver injury in hepatic surgery.

The main weakness of our study was the lack of follow-up after 24 h, which was difficult to implement due to the highly demanding postoperative care. In our experience, the model requires a multidisciplinary team with high experience in hepatobiliary surgery and critical care, as these animals need to be sedated and managed in an intensive care unit similar to what is performed in humans. This limitation, however, does not diminish the validity of the study, as it is important to emphasize that the "Small-for-Flow" syndrome is defined by intraoperative parameters and the present model reproduced all the characteristic hemodynamic alterations and allowed the assessment of relevant clinical and hemodynamic endpoints. Nonetheless, additional studies with a longer follow up will be important to assess the final impact of potential interventions, such as splenic embolization, regenerative preconditioning, and somatostatin infusion.

Conclusion

The porcine hepatectomy model reported here was feasible and reproducible, and it faithfully recreated the pathophysiology of the "Small-for-Size" syndrome and the postoperative liver failure, representing a useful tool for studying their prediction, prevention, diagnosis, and management. The study also suggested that PP is preferable to PBF for prognosis and therapeutic guidance. Importantly, the adequate performance of the model required a multidisciplinary team and the combined evaluation of clinical, laboratory, hemodynamic, and histopathological findings.

Authors Contribution Acquisition of data and drafting the work and final approval and agreement to be accountable for the work: Pablo Lozano, Miguel A. Steiner, Álvaro Morales, Juan Laso, Inma Hernández, Isabel Peligros, Emma Sola, Carlos Carballal, Elena Vara

Acquisition, analysis, and interpretation of data and drafting and revising and final approval and agreement to be accountable for the work: Maitane I. Orue-Echebarria, Javier Vaquero, Cristina J. Lisbona

Conception, design, acquisition, analysis, and interpretation and revising and final approval and agreement to be accountable for the work: José M. Asencio, Jose Á. López-Baena, José L. García Sabrido, Luis Olmedilla

Funding Information This study is supported by a grant of the Sociedad Española de Trasplante Hepático (SETH) to J.M.A. J.V. was supported by a grant from ISCIII-Fondos FEDER "Una manera de hacer Europa" (PI15/1083) from Spain.

Compliance with Ethical Standards

Conflict of Interest The authors declare that they have no conflict of interest.

References

1. Allard M-A, Adam R, Bucur P-O, Termos S, Cunha AS, Bismuth H, et al. Posthepatectomy portal vein pressure predicts liver failure and mortality after major liver resection on noncirrhotic liver. Ann. Surg. 2013; 258: 822–829.
2. Selzner M, Kashfi A, Cattral MS, Selzner N, Greig PD, Lilly L, et al. A graft to body weight ratio less than 0.8 does not exclude adult-to-adult right-lobe living donor liver transplantation. Liver Transpl. 2009; 15: 1776–1782.
3. Kaido T, Mori A, Ogura Y, Hata K, Yoshizawa A, Iida T, et al. Lower limit of the graft-to-recipient weight ratio can be safely reduced to 0.6% in adult-to-adult living donor liver transplantation in combination with portal pressure control. Transplant. Proc. 2011; 43: 2391–2393.
4. Sato Y, Yamamoto S, Oya H, Nakatsuka H, Tsukahara A, Kobayashi T, et al. Splenectomy for reduction of excessive portal hypertension after adult living-related donor liver transplantation. Hepatogastroenterology. 2002; 49: 1652–1655.
5. Shoreem H, Gad EH, Soliman H, Hegazy O, Saleh S, Zakaria H, et al. Small for size syndrome difficult dilemma: lessons from 10 years single centre experience in living donor liver transplantation. World J Hepatol. 2017; 9: 930–944.
6. Nguyen JH, Harnois DM. Incidence and outcome of small-for-size liver grafts transplanted in adult recipients. Transplant. Proc. 2018; 50: 198–201.
7. Nagano Y, Nagahori K, Kamiyama M, Fujii Y, Kubota T, Endo I, et al. Improved functional reserve of hypertrophied contra lateral liver after portal vein ligation in rats. J. Hepatol. 2002; 37: 72–77.
8. Sethi P, Thillai M, Thankamonyamma BS, Mallick S, Gopalakrishnan U, Balakrishnan D, et al. Living donor liver transplantation using small-for-size grafts: does size really matter? J Clin Exp Hepatol. 2018; 8: 125–131.
9. Boillot O, Delafosse B, Méchet I, Boucaud C, Pouyet M. Small-for-size partial liver graft in an adult recipient; a new transplant technique. Lancet. 2002; 359: 406–407.
10. Yagi S, Iida T, Hori T, Taniguchi K, Yamamoto C, Yamagiwa K, et al. Optimal portal venous circulation for liver graft function after living-donor liver transplantation. Transplantation. 2006; 81: 373–378.
11. Troisi R, de Hemptinne B. Clinical relevance of adapting portal vein flow in living donor liver transplantation in adult patients. Liver Transpl. 2003; 9: S36–41.
12. Troisi R, Ricciardi S, Smeets P, Petrovic M, Van Maele G, Colle I, et al. Effects of hemi-portocaval shunts for inflow modulation on the outcome of small-for-size grafts in living donor liver transplantation. Am. J. Transplant. 2005; 5: 1397–1404.
13. Asencio JM, Vaquero J, Olmedilla L, García Sabrido JL. "Small-for-flow" syndrome: shifting the "size" paradigm. Med. Hypotheses. 2013; 80: 573–577.

14. Court FG, Wemyss-Holden SA, Morrison CP, Teague BD, Laws PE, Kew J, et al. Segmental nature of the porcine liver and its potential as a model for experimental partial hepatectomy. Br J Surg. 2003; 90: 440–444.
15. Golriz M, Fonouni H, Nickkholgh A, Hafezi M, Garoussi C, Mehrabi A. Pig kidney transplantation: an up-to-date guideline. Eur Surg Res. 2012; 49: 121–129.
16. Fondevila C, Hessheimer AJ, Taurá P, Sánchez O, Calatayud D, de Riva N, et al. Portal hyperperfusion: mechanism of injury and stimulus for regeneration in porcine small-for-size transplantation. Liver Transpl. 2010; 16: 364–374.
17. Asencio JM, García-Sabrido JL, López-Baena JA, Olmedilla L, Peligros I, Lozano P, et al. Preconditioning by portal vein embolization modulates hepatic hemodynamics and improves liver function in pigs with extended hepatectomy. Surgery. 2017; 161: 1489–1501.
18. Asencio JM, García Sabrido JL, Olmedilla L. How to expand the safe limits in hepatic resections? J Hepatobiliary Pancreat Sci. 2014; 21: 399–404.
19. Mohkam K, Darnis B, Mabrut J-Y. Porcine models for the study of small-for-size syndrome and portal inflow modulation: literature review and proposal for a standardized nomenclature. J Hepatobiliary Pancreat Sci. 2016; 23: 668–680.
20. Xia Q, Lu T-F, Zhou Z-H, Hu L-X, Ying J, Ding D-Z, et al. Extended hepatectomy with segments I and VII as resection remnant: a simple model for small-for-size injuries in pigs. HBPD INT. 2008; 7: 601–607.
21. Kahn D, Hickman R, Terblanche J, von Sommoggy S. Partial hepatectomy and liver regeneration in pigs–the response to different resection sizes. J. Surg. Res. 1988; 45: 176–180.
22. Kaiser GM, Frühauf NR. Method of intracranial pressure monitoring and cerebrospinal fluid sampling in swine. Lab. Anim. 2007; 41: 80–85.
23. Frühauf NR, Radunz S, Grabellus F, Laube T, Uerschels AK, Kaiser GM. Neuromonitoring in a porcine model of acute hepatic failure. Lab. Anim. 2011; 45: 174–178.
24. Dahm F, Georgiev P, Clavien P-A. Small-for-size syndrome after partial liver transplantation: definition, mechanisms of disease and clinical implications. Am. J. Transplant. 2005; 5: 2605–2610.
25. Rahbari NN, Garden OJ, Padbury R, Brooke-Smith M, Crawford M, Adam R, et al. Posthepatectomy liver failure: a definition and grading by the International Study Group of Liver Surgery (ISGLS). Surgery. 2011; 149: 713–724.
26. Qadan M, Garden OJ, Corvera CU, Visser BC. Management of postoperative hepatic failure. J. Am. Coll. Surg. 2016; 222: 195–208.
27. Demetris AJ, Kelly DM, Eghtesad B, Fontes P, Wallis Marsh J, Tom K, et al. Pathophysiologic observations and histopathologic recognition of the portal hyperperfusion or small-for-size syndrome. Am. J. Surg. Pathol. 2006; 30: 986–993.
28. Kelly DM, Demetris AJ, Fung JJ, Marcos A, Zhu Y, Subbotin V, et al. Porcine partial liver transplantation: a novel model of the "small-for-size" liver graft. Liver Transpl. 2004; 10: 253–263.
29. Sainz-Barriga M, Scudeller L, Costa MG, de Hemptinne B, Troisi RI. Lack of a correlation between portal vein flow and pressure: toward a shared interpretation of hemodynamic stress governing inflow modulation in liver transplantation. Liver Transpl. 2011; 17: 836–848.